

# Power-Law Sensitivity To Initial Conditions In Sea Clutter

Jing Hu<sup>1</sup>, Jianbo Gao<sup>1</sup>, and Kung Yao<sup>2</sup>

<sup>1</sup>Department of Electrical and Computer Engineering, University of Florida, Gainesville, FL32611

<sup>2</sup>Electrical Engineering Department, University of California, Los Angeles, LA, CA 90095

Key Words: chaos, power-law sensitivity to initial conditions, sea clutter, target detection

## ABSTRACT

Understanding the nature of sea clutter is crucial to the successful modeling of sea clutter as well as to facilitate target detection within sea clutter. To this end, an important question to ask is whether sea clutter is stochastic or deterministic. In the past decade, Haykin et al. have carried out analysis of some sea clutter data using chaos theory, and concluded that sea clutter was generated by an underlying chaotic process. Recently, their conclusion has been questioned by a number of researchers. To reconcile ever growing evidence of stochasticity in sea clutter with their chaos hypothesis, Haykin et al. have further suggested that the non-chaotic feature of sea clutter could be due to many types of noise sources in the data. To test this possibility, McDonald and Damini have tried a series of low-pass filters to remove noise; but again they have failed to find any chaotic features. While most of these studies are conducted by comparing measured sea clutter data with simulated stochastic processes, we use the direct dynamical test for deterministic chaos developed by Gao and Zheng to analyze 280 sea clutter data measured under various sea and weather conditions. The method offers a more stringent criterion for detecting low-dimensional chaos, and can simultaneously monitor motions in phase space at different scales. However, no chaotic feature is observed from any of these scales. But more interestingly, we find that sea clutter can be conveniently characterized by the new concept of power-law sensitivity to initial conditions (PSIC), which generalizes the defining property for chaotic dynamics, the exponential sensitivity to initial conditions (ESIC). We show that PSIC offers a powerful method for detecting targets within sea clutter.

## 1. INTRODUCTION

Understanding the nature of sea clutter is crucial to the successful modeling of sea clutter as well as to facilitate target detection within sea clutter. To this end, an important question to ask is whether sea clutter is stochastic or deterministic. Since the complicated sea clutter signals are functions of complex (sometimes turbulent) wave motions on the sea surface, while wave motions on the sea surface clearly have their own dynamical features that are not readily described by simple statistical features, it is thus very appealing to understand sea clutter by considering some of their dynamical features. In the past decade, Haykin et al. have carried out

analysis of some sea clutter data using chaos theory [1, 2], and concluded that sea clutter was generated by an underlying chaotic process. Recently, their conclusion has been questioned by a number of researchers [3-9]. In particular, Unsworth et al. [6, 7] have demonstrated that the two main invariants used by Haykin et al. [1, 2], namely the “maximum likelihood of the correlation dimension estimate” and the “false nearest neighbors” are problematic in the analysis of measured sea clutter data, since both invariants may interpret stochastic processes as chaos. They have also tried an improved method, which is based on the correlation integral of Grassberger and Procaccia [10] and has been found effective in distinguishing stochastic processes from chaos. Still, no evidence of determinism or chaos has been found in sea clutter data.

To reconcile ever growing evidence of stochasticity in sea clutter with their chaos hypothesis, recently, Haykin et al. [11] have suggested that the non-chaotic feature of sea clutter could be due to many types of noise sources in the data. To test this possibility, McDonald and Damini [12] have tried a series of low-pass filters to remove noise; but again they have failed to find any chaotic features. Furthermore, they have found that the commonly used chaotic invariant measures of correlation dimension and Lyapunov exponent, computed by conventional ways, produce similar results for measured sea clutter returns and simulated stochastic processes, while a nonlinear predictor shows little improvement over linear prediction.

While these recent studies highly suggest that sea clutter is unlikely to be truly chaotic, a number of fundamental questions are still unknown. For example, most of these studies [3-7] are conducted by comparing measured sea clutter data with simulated stochastic processes. We can ask: can the non-chaotic nature of sea clutter be directly demonstrated without resorting to simulated stochastic processes? Recognizing that simple low-pass filtering does not correspond to any definite scales in phase space, can we design a more effective method to separate scales in phase space and to test whether sea clutter can be decomposed as signals plus noise? Finally, will studies along this line be of any help for target detection within sea clutter?

In this paper, we employ the direct dynamical test for deterministic chaos developed by Gao and Zheng [13] to analyze 280 sea clutter data measured under various sea and weather conditions. The method offers a more stringent criterion for detecting low-dimensional chaos, and can simultaneously monitor motions in phase space at different

scales. However, no chaotic feature is observed from any of these scales. But very interestingly, we find that sea clutter can be conveniently characterized by the new concept of power-law sensitivity to initial conditions (PSIC), which generalizes the defining property for chaotic dynamics, the exponential sensitivity to initial conditions (ESIC). We show that PSIC offers a powerful method for detecting targets within sea clutter.

The remainder of the paper is organized as follows. In Sec. 2, we briefly describe the sea clutter data. In Sec. 3, we first introduce some background knowledge about the chaos theory, so that our study can be accessible to a wider range of readers. Then we study the sea clutter data by employing the direct dynamical test for low-dimensional chaos developed by Gao and Zheng [13]. In Sec. 4, we introduce the general theoretical and computational framework for the PSIC, and apply this concept to detect targets within sea clutter. Finally we summarize our work in Sec. 5.

## 2. SEA CLUTTER DATA

We have obtained 14 sea clutter datasets from a website maintained by Professor Simon Haykin: <http://soma.ece.mcmaster.ca/ipix/dartmouth/datasets.html>.

The measurement was made using the McMaster IPIX radar at the east coast of Canada, from a clifftop near Dartmouth, Nova Scotia. The RF of the radar is 9.39 GHz (and hence a wavelength of about 3 cm). The grazing angle varied from less than  $1^\circ$  to a few degrees. The wave height in the ocean varied from 0.8 m to 3.8 m (with peak height up to 5.5 m). The wind conditions varied from still to 60 km/hr (with gusts up to 90 km/hr). We analyze data of two polarizations, HH (horizontal transmission, horizontal reception) and VV (vertical transmission, vertical reception). Each dataset contains 14 spatial range bins of HH as well as 14 range bins of VV datasets. Therefore, there are a total of 392 sea clutter time series. A few of the range bins hit a target, which was made of a spherical block of styrofoam of diameter 1 m, wrapped with wire mesh. Each range bin data contains  $2^{17}$  complex numbers, with a sampling frequency of 1000 Hz. We analyze the amplitude data. Fig. 1 shows two examples of the typical sea clutter amplitude data without and with target. However, careful examination of the amplitude data indicates that 4 datasets are severely affected by the occasional clipping around the 1.2 amplitude value. This can be readily observed from Figs. 2(a, b). We discard 4 such datasets. Therefore, we analyze a total of 280 sea clutter time series.

## 3. NON-CHAOTIC BEHAVIOR OF SEA CLUTTER

Chaos is also commonly called a strange attractor. Being an “attractor” means the trajectories in the phase space are bounded. Being “strange”, the nearby trajectories, on the average, diverge exponentially fast. The latter property is characterized by the ESIC, and can be mathematically expressed as follows. Let  $d(0)$  be the small separation between two arbitrary trajectories at time 0, and  $d(t)$  be the separation between them at time  $t$ . Then, for true low-

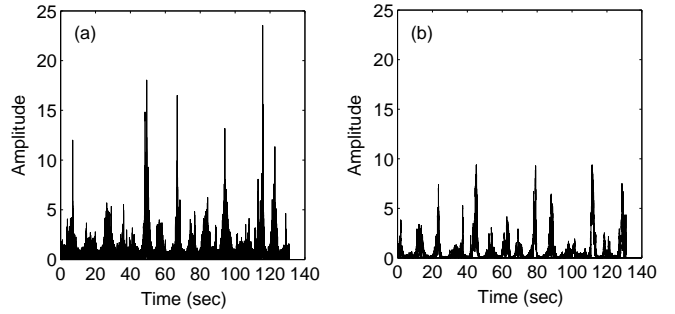


Fig.1 Examples of sea clutter amplitude data (a) without and (b) with target.

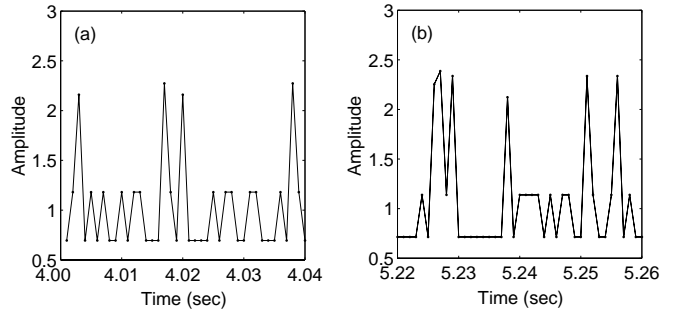


Fig.2 Two short segments of the amplitude sea clutter data severely affected by the occasional clipping around the 1.2 amplitude value.

dimensional deterministic chaos, we have

$$d(t) \sim d(0)e^{\lambda_1 t} \quad (1)$$

where  $\lambda_1$  is positive and called the largest Lyapunov exponent. Due to the boundedness of the attractor and the exponential divergence between nearby trajectories, a strange attractor typically is a fractal, characterized by a simple and elegant scaling law:

$$N(\varepsilon) \sim \varepsilon^{-D}, \quad \varepsilon \rightarrow 0 \quad (2)$$

where  $N$  represents the (maximal) number of boxes, of linear length not larger than  $\varepsilon$ , needed to cover the attractor, and  $D$  is typically a non-integral number called the fractal dimension of the attractor. A non-integral fractal dimension contrasts sharply with the integer-valued topological dimension (which is 0 for finite number of isolated points, 1 for a smooth curve, 2 for a smooth surface, and so on).

Conventionally, it has been assumed that a time series with an estimated positive largest Lyapunov exponent and a non-integral fractal dimension is chaotic. In fact, this is the very assumption that has resulted in the conclusions made by Haykin et al. [1, 2] that sea clutter data is chaotic. However, it has been found that this assumption may not be a sufficient indication of deterministic chaos. Indeed, this is the main message of the studies by [3-7]. Here, we mention an interesting class of stochastic processes, the so-called  $1/f$  processes. Such processes have spectral density

$$s(f) = f^{-(2H+1)} \quad (3)$$

where  $0 < H < 1$  is sometimes called the Hurst parameter. A trajectory formed by such a process has a fractal dimension of  $1/H$ . As we shall explain shortly, with most algorithms of estimating the largest Lyapunov exponent, one obtains a positive number for the “Lyapunov exponent”, and interprets the random process as originating from deterministic chaos.

The above discussions motivate us to employ a more sophisticated method, the direct dynamical test for deterministic chaos [13], to analyze sea clutter data. The method offers a more stringent criterion for low-dimensional chaos, and can simultaneously monitor motions in phase space at different scales. This method was used by Gao et al. [8, 9] to analyze one single set of sea clutter data, and showed that data was not chaotic. In this paper, we will systematically study 280 sea clutter data measured under various sea and weather conditions, and examine whether any chaotic features can be found from these sea clutter data.

Now let us briefly describe the direct dynamical test for deterministic chaos [13]. Given a scalar time series,  $x(1), x(2), \dots, x(N)$ , (assuming, for convenience, that they have been normalized to the unit interval  $[0,1]$ ), one first constructs vectors of the following form using the time delay embedding technique [14]:

$$X_i = [x(i), x(i+L), \dots, x(i+(m-1)L)] \quad (4)$$

with  $m$  being the embedding dimension and  $L$  the delay time. For example, when  $m=3$  and  $L=4$ , we have  $X_1 = [x(1), x(5), x(9)]$ ,  $X_2 = [x(2), x(6), x(10)]$ , and so on. For the analysis of purely chaotic signals,  $m$  and  $L$  has to be chosen properly. This is the issue of optimal embedding (see [13, 15] and references therein). After the scalar time series is properly embedded, one then computes

$$\Lambda(k) = \ln \left( \frac{\|X_{i+k} - X_{j+k}\|}{\|X_i - X_j\|} \right) > \quad (5)$$

with  $r \leq \|X_i - X_j\| \leq r + \Delta r$ , where  $r$  and  $\Delta r$  are prescribed small distances. The angle brackets denote ensemble averages of all possible pairs of  $(X_i, X_j)$  and  $k$  is called the evolution time, in units of the sampling time. A pair of  $r$  and  $\Delta r$  is called a shell. The computation is typically carried out for a sequence of shells. (One should compare Eq.(5) with Eq.(1) to gain a better understanding.) For true low-dimensional chaotic systems, the curves  $\Lambda(k)$  vs.  $k$  for different shells form a common envelope. The slope of the envelope estimates the largest positive Lyapunov exponent. An example is given in Fig. 3(a) for the well-known chaotic Lorenz system. We note the common envelope at the lower left corner of Fig. 3(a). The existence of that common envelope guarantees that a robust positive Lyapunov exponent will be obtained by different researchers no matter which shell they use in the computation, thus ensures determinism. For non-chaotic systems, the common envelope is absent. As an example, Fig. 3(b) shows the  $\Lambda(k)$  vs.  $k$  curves for a set of uniformly distributed random variables. Here, we note there is no common envelope in the lower left corner of Fig. 3(b). We also note, most other algorithms for estimating the largest

Lyapunov exponent is equivalent to compute  $\Lambda(k)$  for  $r < r_0$ , where  $r_0$  is selected more or less arbitrarily, then obtain  $\Lambda(k)/k$ , for not too large  $k$ , as an estimation of the largest Lyapunov exponent. With such algorithms, one can obtain a “positive” Lyapunov exponent for white noises and for  $1/f$  processes. However, this positive number critically depends on the parameter  $r_0$  chosen in the computation, hence, typically is different for different researchers. We thus observe a random element here! With these discussions, it should be clear why  $1/f$  processes may be interpreted as chaotic.

One can expect that the behavior of the  $\Lambda(k)$  curves for a noisy chaotic system lies in between that of the  $\Lambda(k)$  curves for a clean chaotic system and that of the  $\Lambda(k)$  curves for white noise or for  $1/f$  processes. Actually, it has been demonstrated [16] that for a noisy chaotic system, the  $\Lambda(k)$  curves corresponding to different shells separate, and a common envelope can no longer be defined; the separation is larger between the  $\Lambda(k)$  curves corresponding to smaller shells, indicating that the effect of noise on the small-scale dynamics is stronger than that on the large-scale dynamics. The explicit incorporation of scales in the Gao and Zheng's test [13] enables us to simultaneously monitor motions in phase space at different scales. We systematically analyze 280 amplitude sea clutter time series measured under various sea and weather conditions. However, no chaotic feature is observed from any of these scales. Figs. 4(a,b) show examples

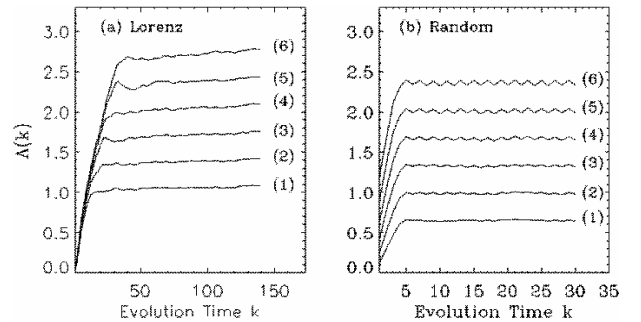


Fig.3  $\Lambda(k)$  vs.  $k$  curves for (a) chaotic Lorenz system and (b) uniformly distributed random noise. Numbers 1, ..., 6 represent different shells [13].

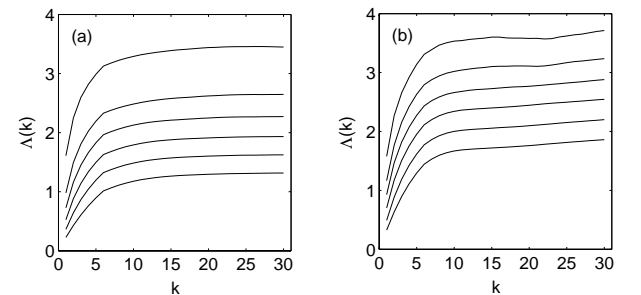


Fig.4 Examples of the  $\Lambda(k)$  vs.  $k$  curves for sea clutter data (a) without and (b) with target.

of the  $\Lambda(k)$  vs.  $k$  curves for the sea clutter amplitude data without and with target of one measurement respectively, with  $m=6$  and  $L=1$ . Similar curves were obtained for other choices of  $m$  and  $L$ . We did not observe a common envelope at any scales. In fact, the results of Fig. 4 are generic among all the 280 sea clutter data analyzed here. Hence, we have to conclude that none of the sea clutter data are chaotic.

#### 4. POWER-LAW SENSITIVITY TO INITIAL CONDITIONS IN SEA CLUTTER

Determining whether the data under investigation is regular, deterministically chaotic, or simply random is a very important issue not only for the successful modeling of sea clutter, but also for many other branches of science and engineering. Conventionally, chaos is characterized by the exponential divergence of nearby trajectories, that is, the exponential sensitivity to initial conditions (ESIC). A bit surprisingly, often ESIC in the rigorous mathematical sense cannot be observed in experimental data (such as sea clutter). Recently, in order to characterize a type of motion whose complexity is neither regular nor fully chaotic/random, the concept of ESIC of deterministic chaos has been generalized to the power-law sensitivity to initial conditions (PSIC) [17, 18].

##### 4.1. THEORY

In the 1-D case, the PSIC is characterized by [17, 18]

$$\xi(t) = \lim_{\Delta x(0) \rightarrow 0} \frac{\Delta x(t)}{\Delta x(0)} = [1 + (1-q)\lambda_q t]^{1/(1-q)} \quad (6)$$

where  $\Delta x(0)$  is the infinitesimal discrepancy in the initial condition,  $\Delta x(t)$  is the discrepancy at time  $t > 0$ ,  $q$  is the entropic index, and  $\lambda_q$  equals  $K_q$ , the generalization of the Kolmogorov-Sinai entropy [17]. When  $t$  is large,  $\xi(t) \sim t^{1/(1-q)}$ . Eq.(6) is the solution to  $d\xi/dt = \lambda_q \xi^q$ .

When  $q \rightarrow 1$ ,  $\xi(t) \rightarrow e^{\lambda t}$ , which is the very definition for the ESIC.

Eq.(6) has been generalized to high-dimensional case[19],

$$\xi(t) = \lim_{\|\Delta x(0)\| \rightarrow 0} \frac{\|\Delta x(t)\|}{\|\Delta x(0)\|} = [1 + (1-q)\lambda_q t]^{1/(1-q)} \quad (7)$$

where  $\|\Delta x(0)\|$  is the infinitesimal discrepancy between two orbits at time 0,  $\|\Delta x(t)\|$  is the distance between the two orbits at time  $t > 0$ . From the experimental data, an orbit can be reconstructed by using Eq.(4).  $q$  is the entropic index, and  $\lambda_q^{(1)}$  is the first  $q$ -Lyapunov exponent, corresponding to the power-law increase of the first principle axis of an infinitesimal ball in the phase space [20].  $\lambda_q^{(1)}$  may not be equal to  $K_q$ . This is understood by recalling that for chaotic systems, the Kolmogorov-Sinai entropy is the sum of all the positive Lyapunov exponents. We conjecture a similar relation may

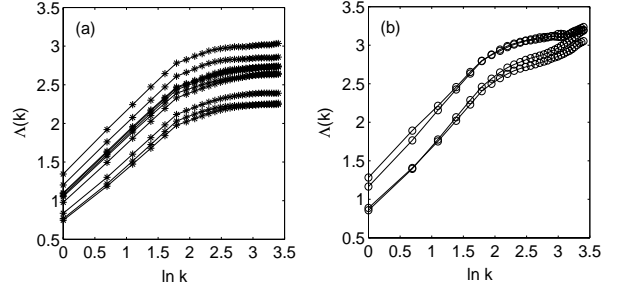


Fig.5 Examples of the  $\Lambda(k)$  vs.  $\ln k$  curves for range bins (a) without and (b) with target. Open circles denote the range bins with target, while \* denote the bins without target.

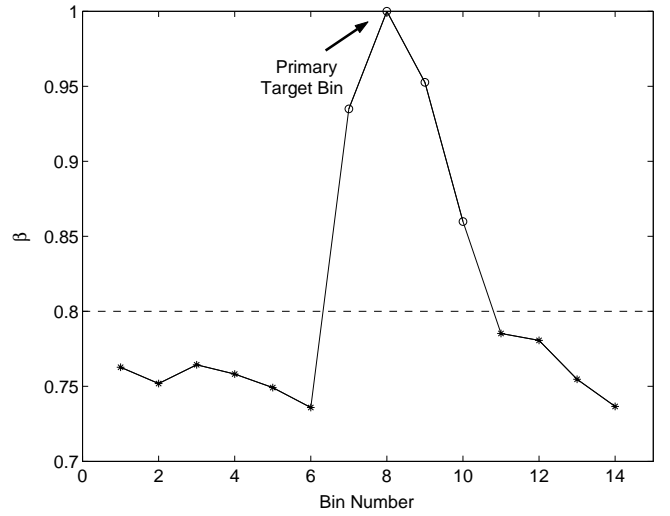


Fig.6 The variation of the  $\beta$  parameter with the 14 range bins. Open circles denote the range bins with target, while \* denote the bins without target.

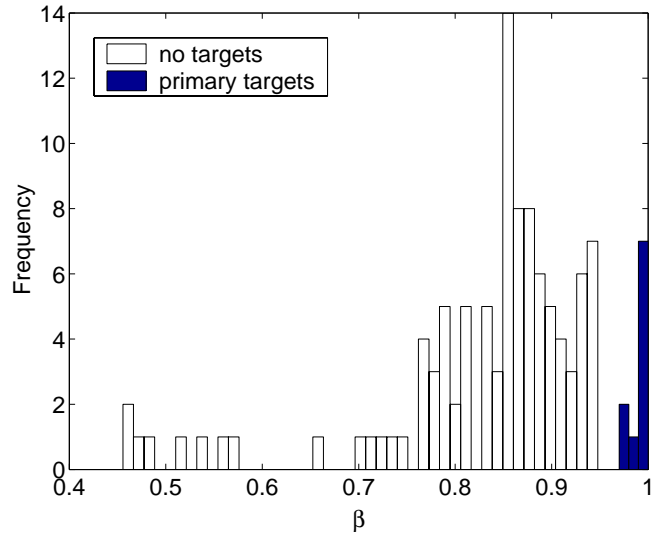


Fig.7 The frequencies of the bins without targets and the bins with primary targets for the HH datasets.

hold between the  $q$ -Lyapunov exponents and  $K_q$ . Then in general,  $\lambda_q^{(1)}$  may not be equal to  $K_q$ . When  $t$  is large, Eq.(7) again gives  $\xi(t) \sim t^{1/(1-q)}$ .

Note that under the above framework, the motion may not be like fully developed chaos, thus not ergodic [20]. In fact, recently we have shown [21] that non-stationary  $1/f^\alpha$  ( $1 \leq \alpha \leq 3$ ) processes can be characterized by PSIC, with  $q = 1 - 2/(\alpha - 1)$  and  $\lambda_q^{(1)} = (\alpha - 1)/2$ . Indeed, in the so-called fractional Brownian motion models[22], an infinitesimal ball and its axes do increase in a power-law fashion, with the exponent being  $(\alpha - 1)/2$ .

Given a finite time series, the condition of  $\|\Delta x(0)\| \rightarrow 0$  cannot be satisfied. In order to find the law governing the divergence of nearby orbits, one thus has to examine how the neighboring points,  $(X_i, X_j)$ , in the phase space, evolve with time, by forming suitable ensemble averages. Notice that if  $(X_{i1}, X_{j1})$  and  $(X_{i2}, X_{j2})$  are two pairs of nearby points, when  $(X_{i1}, X_{j1}) \ll (X_{i2}, X_{j2}) \ll 1$ , then the separations such as  $(X_{i1+k}, X_{j1+k})$  and  $(X_{i2+k}, X_{j2+k})$  cannot be simply averaged to provide estimates for  $q$  and  $\lambda_q^{(1)}$ . In fact, it would be most convenient to consider ensemble averages of pairs of points  $(X_i, X_j)$  that all fall within a very thin shell,  $r_1 \leq \|X_i - X_j\| \leq r_2$ , where  $r_1$  and  $r_2$  are close. These discussions make it clear that  $\xi(t)$  can be computed through the  $\Lambda(k)$  curves [19],

$$\ln \xi(t) \approx \Lambda(k) = \langle \ln \left( \frac{\|X_{i+k} - X_{j+k}\|}{\|X_i - X_j\|} \right) \rangle \sim \beta \ln k \quad (8)$$

where we define  $\beta = 1/(1-q)$ .

#### 4.2. APPLICATION TO TARGET DETECTION

Robust detection of low observable targets within sea clutter is of significant importance to our coastal and national security, to navigation safety, and to environmental monitoring. Here we show how the concept of PSIC can be applied to detect target within sea clutter data. Examples of the  $\Lambda(k)$  vs.  $\ln k$  curves for the range bins without target and those with target of one measurement are shown in Figs. 5(a) and (b), respectively, where the curves denoted by asteroids are for data without the target, while the curves denoted by open circles are for data with the target. We observe that the curves are fairly linear for the first a few samples. Also notice that the slopes of the curves for the data with the target are much larger than those for the data without the target. This feature is shown explicitly in Fig. 6. To better appreciate the variation of the  $\beta$  parameter with the range bins, we normalize  $\beta$  of each bin by the maximal  $\beta$  value of the 14 range bins

within the single measurement. It turns out that the feature shown in Fig. 6 is generically true for all the measurements.

Let us examine if a robust detector for detecting targets within sea clutter can be developed based on the  $\beta$  parameter. We have systematically studied 280 time series of the sea clutter data measured under various sea and weather conditions. To better appreciate the detection performance, we have first only focused on bins with primary targets, but omitted those with secondary targets, since sometimes it is hard to determine whether a bin with secondary target really hits a target or not. After omitting the range bin data with secondary targets, the frequencies for the  $\beta$  parameter under the two hypotheses (the bins without targets and those with primary targets) for HH datasets are shown in Fig. 7. We observe that the frequencies completely separate for the HH datasets. This means the detection accuracy can be 100%.

#### 5. CONCLUSION

In this paper, we have employed the direct dynamical test for deterministic chaos developed by Gao and Zheng [13] to analyze 280 sea clutter data measured under various sea and weather conditions. This test is one of the more stringent criteria for low-dimensional chaos, and can simultaneously monitor motions in phase space at different scales. However, no chaotic feature has been observed from any of these scales. But more interestingly, we have demonstrated that sea clutter can be conveniently characterized by the new concept of PSIC, which generalizes the defining property for chaotic dynamics, the ESIC. We show that PSIC offers a powerful method for detecting targets within sea clutter.

#### REFERENCES

1. S. Haykin and S. Puthusserypady, "Chaotic dynamics of sea clutter", *Chaos*, **7**, 777-802 (1997).
2. S. Haykin, *Chaotic dynamics of sea clutter* (John Wiley) 1999.
3. J.L. Noga, "Bayesian State-Space Modelling of Spatio-Temporal Non-Gaussian Radar Returns", Ph.D thesis, Cambridge University, 1998.
4. M. Davies, "Looking for Non-Linearities in Sea Clutter", *IEE Radar and Sonar Signal Processing*, Peebles, Scotland, July 1998.
5. M.R. Cowper and B. Mulgrew, "Nonlinear Processing of High Resolution Radar Sea Clutter", *Proc. IJCNN* **4**, pp.2633 (1999).
6. C.P. Unsworth, M.R. Cowper, S. McLaughlin, and B. Mulgrew, "False detection of chaotic behavior in the stochastic compound k-distribution model of radar sea clutter", *Proc. 10th IEEE Workshop on SSAP*, August 2000, pp. 296-300.
7. C.P. Unsworth, M.R. Cowper, S. McLaughlin, and B. Mulgrew, "Re-examining the nature of sea clutter", *IEE Proc. Radar Sonar Navig.*, **149**, pp. 105-114 (2002).
8. J.B. Gao and K. Yao, "Multifractal features of sea clutter", *IEEE Radar Conference 2002*, Long Beach, CA, April, 2002.

9. J.B. Gao, S.K. Hwang, H.F. Chen, Z. Kang, K. Yao, and J.M. Liu, "Can sea clutter and indoor radio propagation be modeled as strange attractors?", *The 7th Experimental Chaos Conference*, San Diego, USA, August pp. 25-29, 2002.
10. P. Grassberger and I. Procaccia, "Measuring the strangeness of the strange attractor", *Physica D*, **9D**, pp.189-208 (1983).
11. S. Haykin, R. Bakker, and B.W. Currie, "Uncovering nonlinear dynamics-the case study of sea clutter", *Proc. IEEE* **90**, 860-881 (2002).
12. M. McDonald and A. Damini, "Limitations of nonlinear chaotic dynamics in predicting sea clutter returns", *IEE Proc-Radar Son Nav*, **151**, pp. 105-113 (2004).
13. J.B. Gao and Z.M. Zheng, "Direct dynamical test for deterministic chaos and optimal embedding of a chaotic time series", *Phys. Rev. E*, **49**, 3807 (1994).
14. F. Takens, in *Dynamical Systems and Turbulence, Lecture Notes in Mathematics*, Vol. **898**, edited by D.A. Rand and L.S. Young (Springer-Verlag, Berlin) 1981, pp. 366.
15. J.B. Gao and Z.M. Zheng, "Local exponential divergence plot and optimal embedding of a chaotic time series", *Phys. Lett. A* **181**, 153 (1993).
16. J.B. Gao, C.C. Chen, S.K. Hwang, and J.M. Liu, "Noise-induced chaos", *Int. J. Mod. Phys. B* **V13**, 3283-3305 (1999).
17. C. Tsallis, A.R. Plastino, and W.-M. Zheng, "Power-law sensitivity to initial conditions – new entropic representation", *Chaos, Solitons, & Fractals* **8**, 885-891 (1997).
18. M.L. Lyra and C. Tsallis, "Nonextensivity and multifractality in low-dimensional dissipative systems", *Phys. Rev. Lett.*, **80**, 53-56 (1998).
19. J.B. Gao, W.W. Tung, Y.H. Cao, J. Hu, and Y. Qi, "Power-law sensitivity to initial conditions in a time series with applications to epileptic seizure detection", *Physica A* (in press).
20. J.P. Eckmann and D. Ruelle, "Ergodic theory of chaos and strange attractors", *Rev. Mod. Phys.*, **57**, 617-656 (1985).
21. J.B. Gao, J. Hu, W.W. Tung, Y.H. Cao, and Y. Qi, to be submitted to *Phys. Rev. E*.
22. B.B. Mandelbrot, *The Fractal Geometry of Nature* (San Francisco: Freeman, 1982).